In-situ Observation of Texture & Microstructure Evolution during Rolling and Globularisation of Ti-6Al-4V

J.L.W. Warwick[a], N.G Jones[a], I. Bantounas[b], M. Preuss[c], D. Dye[a,*]

[a]*Dept. Materials, Royal School of Mines, Imperial College, Prince Consort Road, South Kensington, London SW7 2BP, UK*
[b]*Physical Sciences & Engineering Division, KAUST, Thuwal 23955-6900, Kingdom of Saudi Arabia*
[c]*Manchester Materials Science Centre, The University of Manchester, Grosvenor Street, Manchester M1 7HS, UK*

Abstract

The evolution of texture in β-annealed Ti-6Al-4V during α-β rolling and so-called recrystallisation annealing has been examined using synchrotron X-ray diffraction and *ex-situ* characterisation. During rolling, the initial α (0002) texture softens and the colony α becomes kinked. During globularisation, the texture strengthens as highly strained (and hence misoriented) areas of the laths disappear and this strengthening continues once coarsening of the primary α becomes dominant. At shorter heat treatment times the α_s laths that form on cooling do so with a range of variant-related orientations to the β, but at longer annealing times this α_s takes on the orientation of the surrounding α_p. The implications for the mechanical performance of macrozone-containing bimodal Ti-6Al-4V material are discussed.

Keywords: Titanium alloys, Ti-6Al-4V, Synchrotron, Texture, Plastic deformation

1. Introduction

Ti-6Al-4V has been used extensively in both static and rotating components of gas turbine engines for the last 50 years. It also contributes to 80-90% of titanium usage on airframes including the fuselage, nacelles, landing gear, wing and empennage [1]. The initial lamellar microstructure associated with as-cast ingots may promote resistance to fatigue crack growth and high temperature creep but suffers from significant decreases in fatigue crack initiation resistance compared to the more desirable globular primary α (α_p) microstructures [2]. Thermomechanical processing to obtain globular product in $\alpha + \beta$ alloys such as Ti-6Al-4V involves a series of hot working and heat treatment steps, which break down the transformed microstructures developed during initial ingot cooling.

The possible mechanisms by which lamellar microstructures globularise and coarsen into a globular α_p morphology has been studied by various investigators [3–8]. Initial work by Weiss et al. identified two different boundary splitting mechanisms by which lamellar microstructures globularise. They found that boundaries are formed across individual alpha lamellae either due to intense local shear or as a result of dynamic recovery/recrystallisation with β subsequently penetrating the boundary via diffusion [7]. To summarise, the globular α_p grains are formed as a result of deformation and dynamic recovery/recrystallisation of initially course lamellae, whereas the secondary α_s colonies are inherited from the transformation of the β matrix during cooling, which has been reported to follow the Burgers relationship (Eq. 1) [9]. Thus, it is reasonable to assume that α_p and α_s textures developed during thermomechanical processing will be different. A number of different methods have been proposed for the the separation of α_p and α_s textures, which is complicated by the fact that they share the same crystal structure and lattice parameters [9–11].

$$\begin{aligned} \{110\}_\beta \| (0001)_\alpha \\ \langle 111\rangle_\beta \| \langle 11\bar{2}0\rangle_\alpha \end{aligned} \tag{1}$$

Whilst microstructure remains the dominant and most well established factor in determining mechanical properties, it is well documented that strong crystallographic texture can develop during processing. Due to the anisotropic nature of the α phase and its resultant effect on service properties, such as fatigue resistance, a significant research effort has been conducted in the field [12–14].

In recent years, its has been found that titanium alloys very often possess large regions of similarly orientated grains, otherwise known as macrozones, as a result of initial ingot processing. A number of hypotheses have been suggested for the formation of these zones; the concern that these zones behave as single microstructural units drives research in the area. These microtextured regions have been shown to act as sites of multiple initiating cracks. These cracks then coalesce, acting effectively as one large crack, equal to the dimensions of the macrozone [15]. It has been reported that these zones can span several millimetres [16]. Current research therefore suggests that microtexture rather than microstructure can be critical to in-service lifetimes [17].

However, most of the efforts to understand the mechanisms of globularisation have focused on monotonic deformation involving uniaxial compression, tension or simple torsion, whilst

*Corresponding author
Email address: david.dye@imperial.ac.uk (D. Dye)

most commercial mill product employs multi-pass rolling operations with intermittent reheats. Thus, the correlation between laboratory observations and commercial production may be difficult.

The present paper aims to examine how the final microstructure, macro- and microtexture develop during multi-pass cross rolling and subsequent recrystallisation heat treatment. *In-situ* synchrotron X-ray diffraction is employed to examine how the texture develops during recrystallisation at temperature in both the α and β phases. The α_p and α_s textures measured using EBSD are separated on the basis of the composition of the two microstructural forms.

2. Experimental

2.1. Material and Processing

The material used in this investigation was received as a 21 mm thick cross-rolled (XR) plate of Ti-6Al-4V supplied by Timet UK Ltd., Waunarlwydd, Swansea, Wales, with composition given in Table 1. The plate had been produced from a double VAR melted ingot, forged in the β phase field and rolled in the $\alpha + \beta$ phase field to a plate product. The plate was then subjected to a creep-flattening treatment after rolling. Samples measuring 40mm $\times$ 40mm were wire electro discharge machine (EDM) from the as-received plate, coated in Deltaglaze 3418 and subjected to a β annealed at 1020 °C for 20 min followed by an air cool.

These were then hot rolled at 950 °C in six passes with alternating 90° rotations between each pass, Table 2 and Figure 1. Intermediate 5 min reheats were employed, along with air cooling after the final pass, to simulate industrial production. The roll surface speed was 150 mm s^{-1}, and 250 mm diameter rolls were used (approx. 11.5 rpm). Necessarily, there will have been substantial die chill during rolling, particularly during the final passes. Because the sample width / height was only around 2, in the initial passes perfectly plane strain conditions probably were not achieved.

Samples were then recrystallised at 950 °C for up to 16 h and air cooled. 950 °C corresponds to an α volume fraction of $\sim$ 50%. All micrograph's and texture measurements are taken from the mid-plane of the as-received and rolled plate.

Table 2: Rolling process schedule performed at Manchester University, UK. "Reduction" here refers to the nominal strain, *i.e.* the change in height divided by the initial height.

	Height [mm]	Reduction	Total Reduction
Initial	21.0	-	-
Pass 1	18.9	0.1	0.1
Pass 2	16.8	0.1	0.2
Pass 3	13.65	0.15	0.35
Pass 4	10.5	0.15	0.5
Pass 5	7.2	0.157	0.657
Pass 6	3.9	0. 157	0.814

Fig. 1: Initial β annealed and as-rolled samples examined.

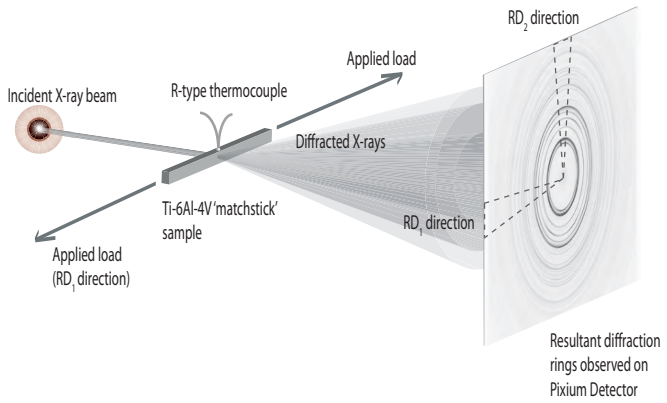

Fig. 2: Schematic of the experimental setup used to perform *in-situ* texture measurements.

2.2. In-situ globularisation texture characterisation

Synchrotron X-ray diffraction (SXRD) texture measurements were carried out on ID15B beamline at the European Synchrotron Radiation Facility (ESRF), Grenoble, France. Matchstick (50x50x1 mm) samples were taken from the 50% rolled (4 passes) material. The beam passed through 1 mm of material, operating with 500×500 µm monochromatic incident beam (λ = 0.1427Å) and therefore a diffraction volume of 0.25mm^3. An R-type thermocouple was spot welded directly above the diffraction volume for accurate control of temperature. Resistive heating was employed using a ElectroThermal Mechanical Tester (ETMT), to a temperature of 950 °C, to simulate the final industrial recrystallisation treatment applied after $\alpha + \beta$ working (Fig. 2). During the heat treatment, complete Debye-Scherrer diffraction rings were collected using a Pixium 4700 area detector. Data was collected every 5 s during heating, every 15 s during the age and every 5 s during cooling. The heating and cooling rates applied were 1°Cs^{-1}.

To evaluate the texture, integrated intensities were calculated every 15° using Fit2D [18]. The resulting 24 spectra were refined simultaneously using a least-squares Rietveld method implemented in the program MAUD [19]. An EWIMV (Williams-Imhof-Matthies-Vinel) algorithm was used to determine the orientation distribution function (ODF), utilising the results of a Le Bail refinement as input. Extended descriptions of this procedure have previously been published [20–22].

2.3. Ex-situ texture characterisation

Supplementary microtexture crystal orientation maps (COM's) were obtained using electron back-scattered diffrac-

Table 1: Measured chemical composition data (wt.%) for material supplied by Timet, UK.

	C	Al	Fe	N	O	H	Ti	V	B	Y	OE
XR Plate	0.005	6.61	0.18	0.0045	0.22	0.004	Balance	4.15	<0.001	<0.001	<0.05

tion (EBSD) on a LEO Gemini 1525 FEGSEM. Preparation of selected samples involved conventional silicon carbide grinding followed by electropolishing in a solution of 15ml perchloric acid(HCl_4), 147.5ml methanol (CH_3OH) and 175ml butan-1-ol (C_4H_9OH) at −35 °C with 30V applied. Simultaneous local Kikuchi patterns and chemical composition data were collected using EBSD and EDS using the Oxford Instruments Channel5 software. In-house automated software has been developed to separate α_p and α_s texture components utilising the technique suggested by Salem [11]. In this method, the α_p that formed at temperature is distinguished from the α_s that forms from the β on the basis of the difference between the Al and V contents, using the minima in the composition-frequency Gaussian curves.

Macrotexture measurements were performed using the back reflection technique with CuK_α radiation on a Panalytical X'Pert Pro MPD diffractometer (XRD). All measurements were taken from the RD_1-RD_2 plane. A complete ODF was calculated using measurements from the $\{10\bar{1}0\}$, $\{0002\}$, $\{10\bar{1}1\}$, $\{10\bar{1}2\}$, $\{11\bar{2}0\}$ peaks via the software tool popLA [23] using the WIMV method. All XRD pole figures were plotted using monoclinic symmetry and the equal area projection. Defocus and background corrections were applied from a calibration measurement using an untextured powder Ti-6Al-4V sample.

The prior-β colony size found in this material was, at maximum, around 500 µm in diameter and around 20 µm in the sample thickness direction (ellipsoidal, with the short axis in the plate normal direction). Therefore in the SXRD measurements around 100 colonies were sampled, because the matchstick vertical direction was the plate normal. Not every grain will have contributed to the diffraction measurements, which correspond to only the outermost ring of each incomplete pole figure for each peak. In comparison, the laboratory X-ray texture measurements sampled the texture from the plate normal direction, and therefore with a 5×5 mm beam measured every one of approx. 150 colonies. EBSD microtexture measurements, in contrast, were obtained from only a few colonies, but allow local texture variations to be examined.

3. Results and Discussion

3.1. As-received

The initial microstructure and concomitant equal area pole figures obtained by laboratory X-ray diffraction and Electron backscattered diffraction (EBSD) can be seen in Fig. 3 and Fig. 4. The initial microstructure possessed an α_p grain size of $\sim 20 \pm 4$ µm, with intergranular retained β which formed during slow cooling from the $\alpha + \beta$ processing temperature. This slow cool promotes α_p growth without the decomposition of the β matrix. Both the lab. X-ray and EBSD texture measurement techniques show very similar results with the basal (0001) plane normals lying in the primary rolling (RD_1) and secondary rolling (RD_2) directions, which is consistent with previous work on a similar product [24], although the EBSD measurements of course suffer from poorer sampling statistics. Fig. 3 shows multi-surface crystal orientation maps (COM's) taken from rolling direction 1 (RD_1), rolling direction 2 (RD_2) and the normal (ND) surfaces. Each map is inverse pole figure (IPF) coloured with respect to RD_1. The pole figures are represented consistently with the RD_1 direction aligned with the y-axis and the RD_2 direction aligned with the x-axis of the pole figure.

Both the prior β and α_p grains were elongated from the rolling process, with their shortest dimension in the ND direction. Therefore the EBSD measurement from the ND face showed equiaxed grains and sampled the fewest grains, whereas the RD_1 and RD_2 measurements sampled more grains providing more representative pole figures and revealing the true grain morphology. This emphasises the utility of examining deformed materials in more than one orientation.

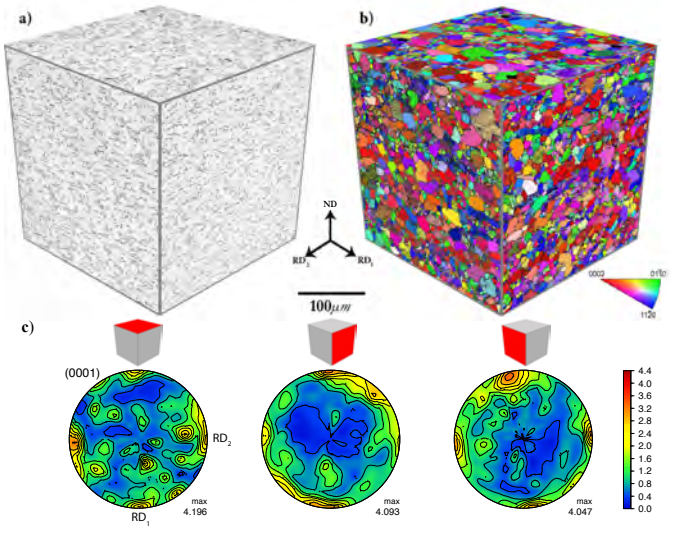

Fig. 3: The as -received microstructure obtained from optical microscopy, (a), and examined using EBSD, (b) and (c).

3.2. β-anneal

The microstructure and pole figures produced as a result of β annealing can be seen in Fig. 4. The initial α microstructure is completely lost during the treatment. The resulting microstructure consists of a mixture of colony α and basketweave α lamellae, with a layer of grain boundary α decorating the prior β grain boundaries. The prior β grains are found to be ~500 µm in size with an α colony size ranging from 50 µm to 250 µm. The initial (0002) texture in the RD_1 and RD_2 directions is generally preserved from the as-received material

but there is an additional 45° texture component produced by the $\alpha \rightarrow \beta \rightarrow \alpha$ variant selection process. It is also apparent, because the 45° texture component is weaker than the remaining original component, that a degree of texture memory exists - less randomisation is observed than might naively be expected. It has been reported that in two-phase Ti-6Al-4V, the nucleation of new β grains from the α matrix which follow the Burgers orientation relationship (OR) is thermodynamically less favourable than growth of existing residual β-phase in the room temperature material [22, 25–27]. However, on cooling from the β phase field (i.e. the $\beta \rightarrow \alpha$ transformation), some new α orientations are observed to adhere to the Burgers OR. Its is therefore apparent that β-annealing Ti-6Al-4V does not result in texture randomisation, but does yield a microstructure conducive to globularisation of the α-phase [28, 29].

3.3. Thermomechanical processing

The as-rolled microstructures and concomitant pole figures are summarised in Fig. 4. On air cooling from the rolling temperature, the α laths thicken, leaving ligaments of β in between. The 20% rolled material still shows traces of the grain boundary intergranular α, and has begun to show some kinking of the laths. At 50% deformation the lath kinking has become quite apparent while some areas of larger α grains with less linear grain boundaries due to dynamic recrystallisation also begin to be more apparent. After 80% deformation these regions become quite pronounced and are observed to be associated with the prior-β grain triple points. Over the course of rolling the α texture also gradually weakens (returns towards a random orientation distribution), as observed by Lütjering [2] for intermediate $\alpha + \beta$ deformation temperatures; at lower temperatures a more pronounced {0002} transverse texture is observed whereas at higher temperatures a texture characteristic of the β phase is produced. However, in the present case this texture weakening ceased after approx. 50% strain, around the same level that dynamic recrystallisation started to become significant.

The evolution of the air-cooled material during 950 °C heat treatment of the 50% rolled material is shown in Figure 5. Such a heat treatment is often termed 'recrystallisation annealing,' but it essentially composes two processes. First, the kinked α laths break up into spherical primary α (α_p) in the globularisation process. Subsequently, growth in the α_p is observed, presumably accompanied by an overall reduction in defect density (recovery). This process is observed as follows: after 2 h breakup of the kinked laths has already occurred to form primary α grains; on cooling, secondary lath α has formed from the β in between the α_p. In some prior α colonies (inset), complete globularisation to equiaxed α_p was not observed in the 2 h recrystallised specimen, leaving elongated α_p instead. This is likely to be due to the original colony morphological and crystallographic orientation receiving less strain and less lath kinking due the rolling process, and hence having a lower dislocation density to initiate lath globularisation. We will return to this topic subsequently. At longer annealing times, Figure 5, the globularisation process is complete and limited growth of the α_p is observed. As heat treatment proceeds (i) strengthening of the (0002) α texture is observed. In addition, (ii) in

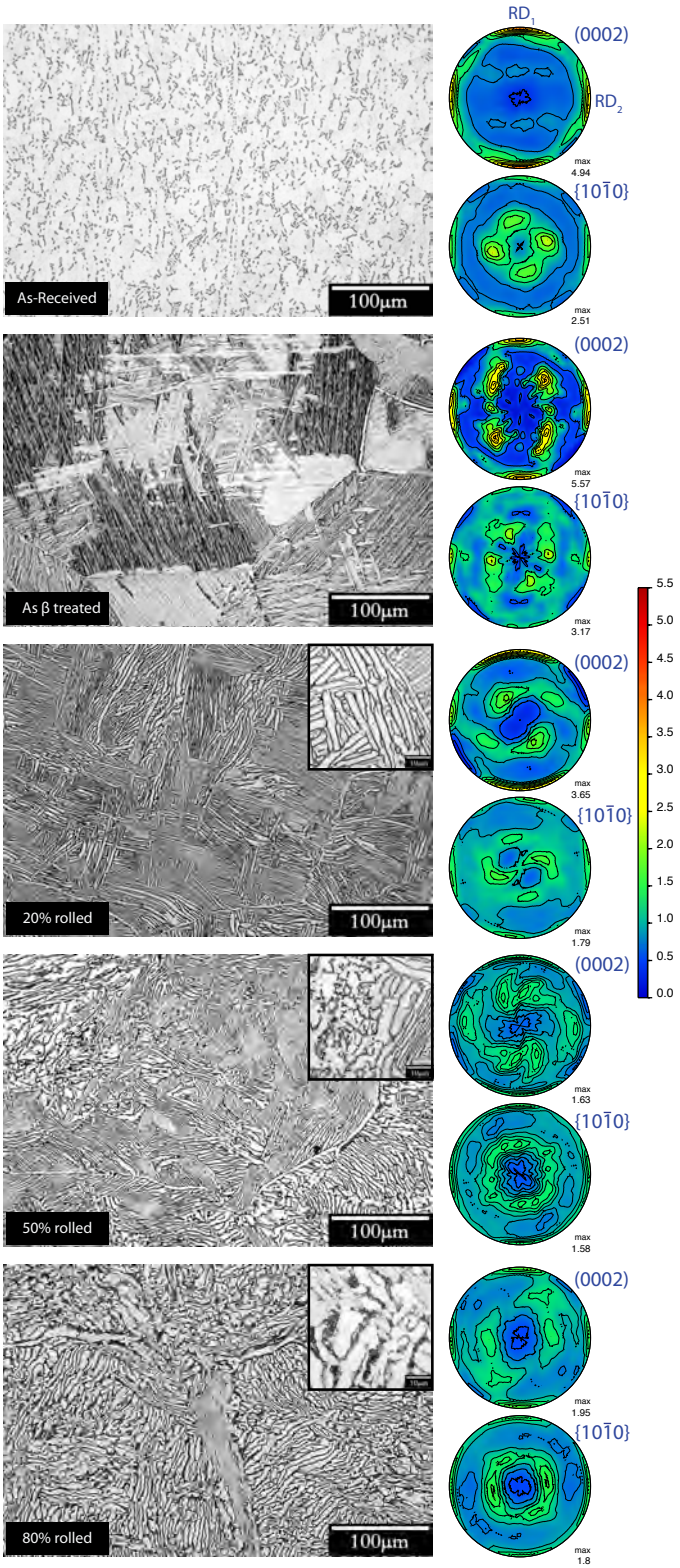

Fig. 4: The as-received, as-β treated and hot rolled microstructures, along with the macroscopic textures obtained by lab. X-ray diffraction. The scale bars in the inset micrographs are 10 μm.

the 20% rolled sample some of the 45°texture component from the Burgers OR is observed, but at longer times this component becomes much less apparent. It is these two observations (i)-(ii) that will be of most interest in understanding how the microstructure and texture evolve during the 'recrystallisation annealing' step.

3.4. In-situ texture evolution during recrystallisation annealing

When considering *in situ* texture measurements performed using area detectors by synchrotron X-ray diffraction, it is important to establish whether enough prior-β grains were sampled to accurately reconstruct the macroscopic texture. This is a function of the beam divergence, sampling volume and the number of diffraction orientations sampled. Each ring measures the edge of a pole figure from the RD_1 around to the TD orientation, with the entire orientation distribution being reconstructed in the EWIMV analysis from the 8 rings measured. Therefore Figure 6 shows the comparison between the lab. X-ray and synchrotron reconstructed pole figures in the initial as-received condition; it is apparent that the data are in reasonable agreement. The synchrotron X-ray diffraction measurements were made on multiple rings without sample rotation and therefore the textures shown are reconstructed from sampling of rings from the RD_1-RD_2 great circle. It is apparent that the reconstruction in the α phase produces a level of artefact near the ND direction, which many authors suppress by applying symmetry; this is viewed as inappropriate and therefore this has not been performed in the present work.

The evolution of the texture in the 50% rolled sample is illustrated on heat-up, recrystallisation annealing for 8 h and cool-down in Figure 7 (animation online). The β phase texture is also reconstructed, which is possible because of the low background in this measurement and the Reitveld refinement performed rather than single peak measurements. Before discussing the substance of Figre 7, we first develop some summary measure of the evolution and comparison to *ex situ* measurements. This evolution is quantitively summarised in Figure 8. Kearns' factors describe the fraction of the α (0002) poles that are in the ND and two RD directions, according to Equation 2 [30].

$$f = \frac{\int_0^{\pi} I_\vartheta \cos^2\vartheta \sin\vartheta \, \mathrm{d}\vartheta}{\int_0^{\pi} I_\vartheta \sin\vartheta \, \mathrm{d}\vartheta} \qquad (2)$$

Here, I_ϑ is the average pole figure intensity at an angle ϑ from the sample normal. The function I_ϑ is used by Kearns and is equivalent to the integral $\int_0^{2\pi} I(\phi,\vartheta)\mathrm{d}\phi$ over the pole figure intensity $I(\phi,\vartheta)$ [30].

The Kearns' factors measured throughout processing are approximately constant at 0.31-0.34 in the ND, 0.32-0.34 in RD_2 and 0.34-0.37 in RD_1. Thus the overall fractions of the (0002) in the different major directions remain nearly constant throughout the $\alpha - \beta$ rolling and recrystallisation processes. However, Kearns' factors don't attempt to measure the strength of the macrotexture and at such relatively moderate strains in a co-deforming material dominated by slip, large scale texture reorientation would not be expected.

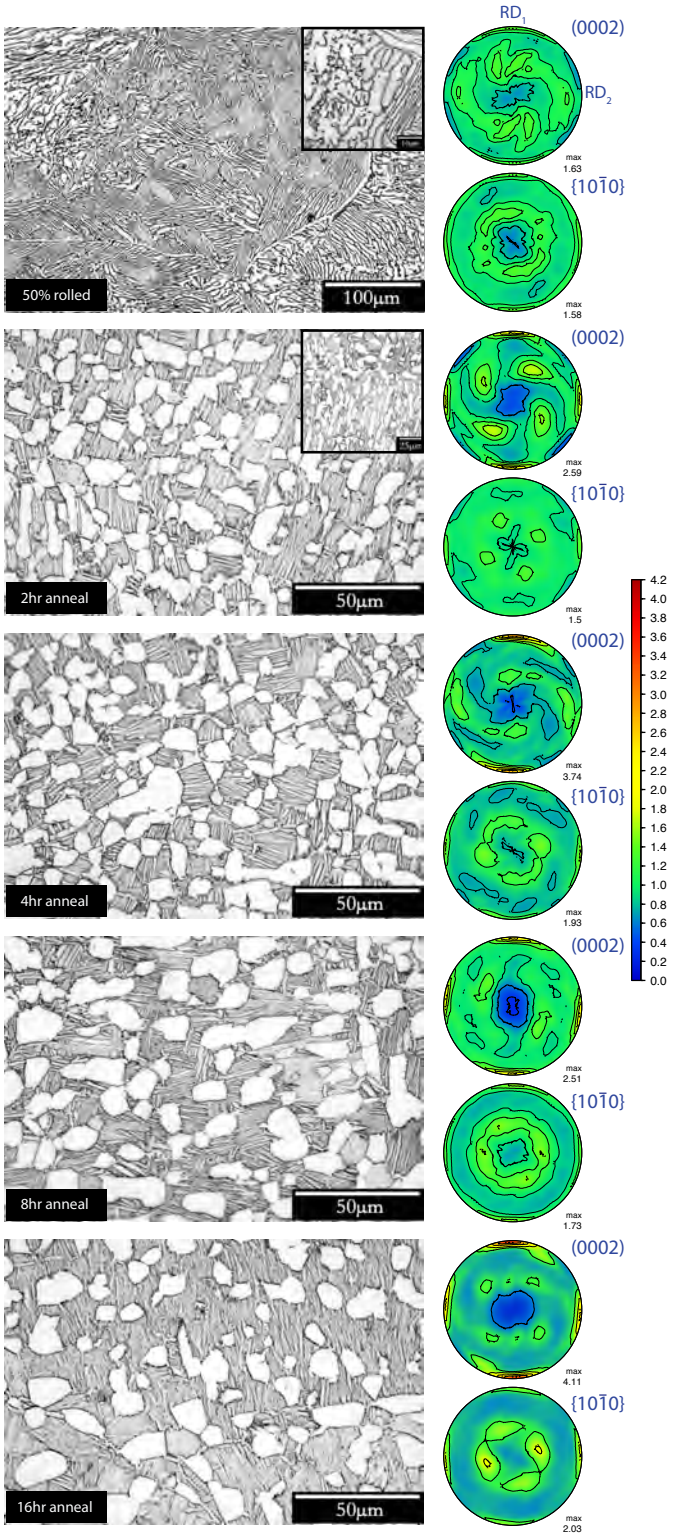

Fig. 5: Evolution of the microstructure and texture (lab. X-ray) of the 50% rolled sample during 950 °C recrystallisation heat treatment. In the inset figures, the scale bars are 10 μm in the as-rolled and 20 μm is the 2 h anneal.

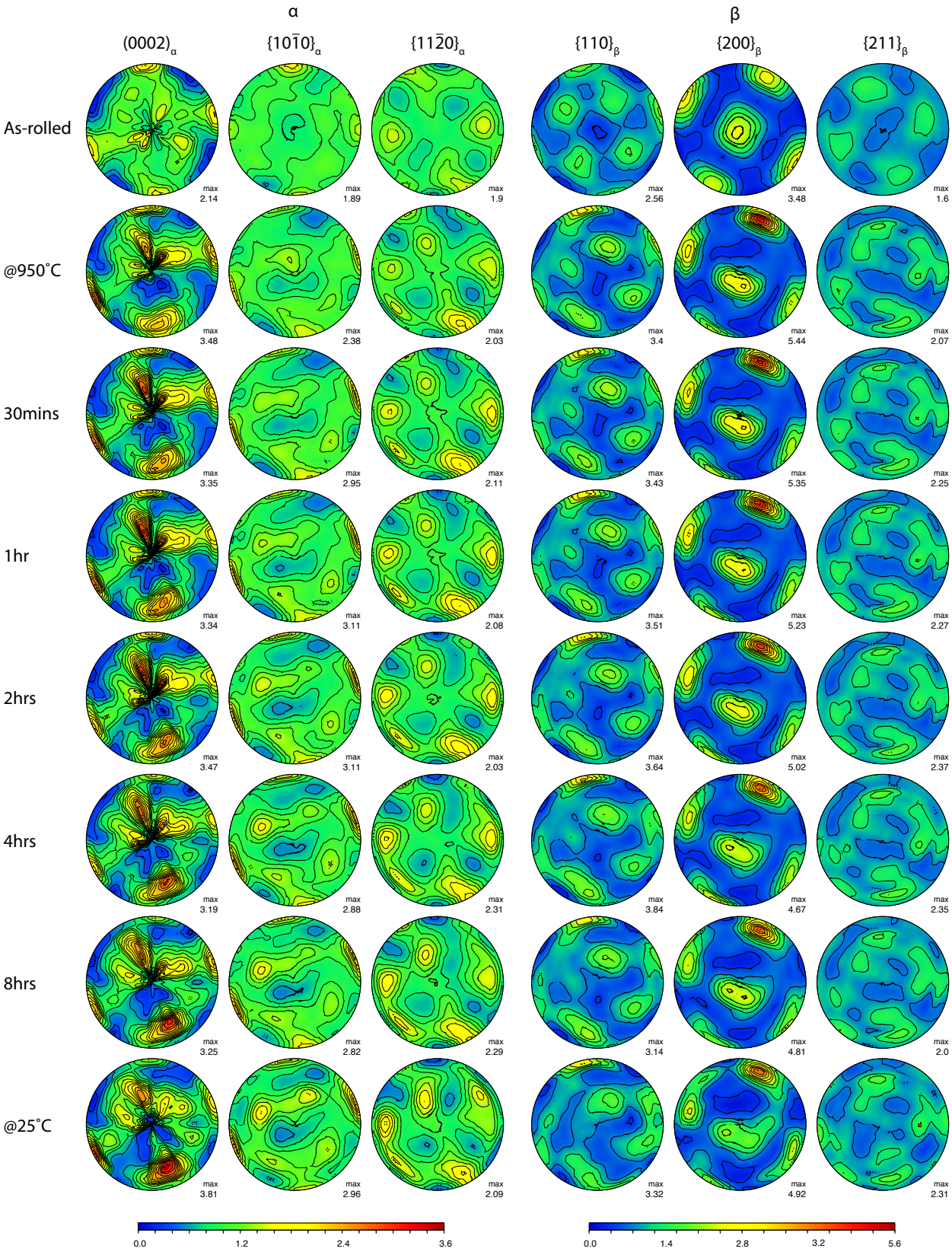

Fig. 7: α and β pole figures reconstructed from the *in situ* synchrotron diffraction measurements before, during and after recrystallisation annealing of the 50% rolled material. RD_1 corresponds to the 12 O'clock position, RD_2 to the 9 O'clock position and the ND direction to the centre of the pole figures. Measurements were made in the RD_1-RD_2 great circle from the first 10 diffraction rings in the α phase.

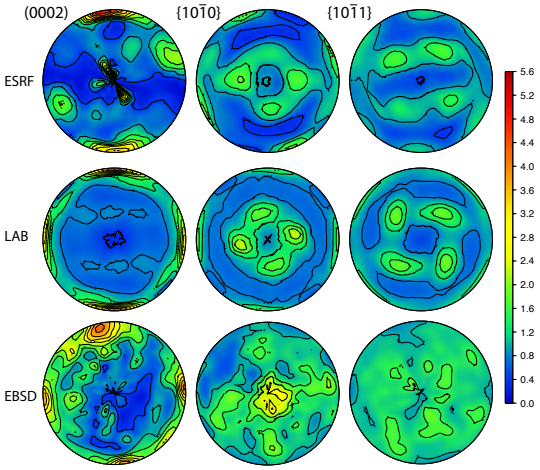

Fig. 6: Comparison of the textures of the as-received material produced from the synchrotron X-ray diffraction reconstruction, from Lab. X-ray texture measurement and by EBSD scanning (300×300 μm scan area, RD_2 face, c.f. Fig. 3).

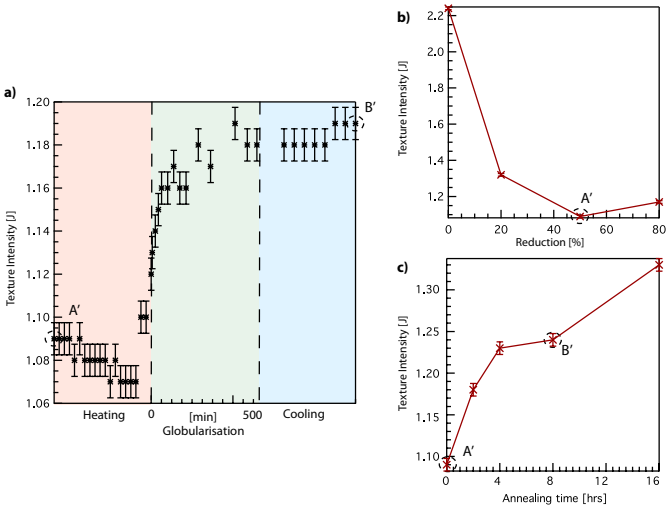

Fig. 8: Evolution of the texture intensity J of the α phase during (a) recrystallisation annealing *in situ* SXRD, (b) after rolling and air cooling (lab. XRD) and (c) after annealing and cooling *ex situ* (lab XRD). The points A′ and B′ correspond to different measurement techniques on the same 50% rolled material.

The texture strength J describes the root mean square of the orientation distribution, for which spherical harmonic texture functions can be described according to

$$J = 4\pi^2 \sqrt{2} \sum_{l=1}^{\infty} \sum_{m=-1}^{1} \sum_{n=-1}^{1} W_{lmn}^2 \qquad (3)$$

where W_{lmn} are the spherical harmonic coefficients. Ex-situ lab, X-ray texture strengths are presented in Figure 8 for the rolled and interrupted annealing samples; the points marked A′ and B′ correspond to lab X-ray and synchrotron measurements in identical samples and are in reasonable agreement. The use of two techniques and of the whole-texture summary index J therefore allows the scatter in the reconstructed texture maxima in Figure 7 to be discounted.

Returning to Figure 7, during initial heating of the 50% rolled material the β fraction increases and the {110} texture component near-RD_1 strengthens slightly, corresponding to the dissolution of the corresponding (0002) α in the same location; it is also apparent that the β texture peaks are broader and more intense that the α. On heating, dissolution of the α_s results in a strengthening of the α texture, as the variant-related α_s is less textured overall than the α_p. Over the first 2 h at temperature, the α texture component near-ND strengthens quite significantly, while the β softens. During this period, regions of the α laths that are kinked, have high dislocation density and are away from the Burgers OR with respect to the surrounding β grain disapper as the grain re-formation process of globularisation occurs, therefore giving rise to the α texture strengthening observed, although this is the reconstructed area of the pole figure where least confidence can be sustained.

Between 2 and 8 h spheoidisation / globularisation of the α_p completes and coarsening (change in size at approximately constant volume fraction) becomes dominant. In this period the near-ND (0002) α texture component softens at the expense of the near-RD_1 and RD_2 components; and this strengthening of the RD-type components is in the measurement region and so this observation can be stated confidently. This change may be due to restoration of the α / β interface orientation relationship as accumulated interface dislocations are removed, although this interpretation is speculative.

On cooling, the α_s that now forms from the β results in a strengthening of the texture, following the orientation of the α_p rather than the weakening that would be expected were the heating step simply reversed. Thus the 45°component from variant selection is not now observed; similarly in the β phase those {110} components disappear during annealing. This strongly suggests that restoration of the α-β interface relationship is driving microstructural evolution during the recrystallisation process, and that then on cooling the α_s that forms conforms to the parent α_p orientations. This interpretation is consistent with the *ex situ* measurements of Moustahfid et al [31] but disagrees with the interpretation of Divinski et al [32] who suggested that the supression of the 45°component was somehow driven by a mechanical supression of out-of-plane components in the sheet.

Figure 8(b) shows that rolling results in a marked reduction in texture intensity. During *in situ* heat treatment, Figure 8(a), a slight decrease (in the range of scatter) in texture strength in the α phase is observed during α dissolution during heating, followed by a significant increase in the final stages of heating, followed by a gradual strengthening of the α texture during globularisation in the initial 2 h and removal of the ND texture component between 2 and 8 h, after which the texture strength is preserved on cooling. For comparison, the *ex-situ*, air cooled lab. X-ray measurements are also shown, which would be harder to interpret without the benefit of the *in situ* measurements. These also show an increase in texture strength after cooling for short-duration annealing treatments, a plateau at intermediate times and then an increase in texture strength on cooling after 16 h. The plateau is felt to be a consequence of the change from the α_s taking on many variant orientations to just the orientation of the surrounding α_p.

3.5. Microstructure and microtexture evolution

The rolled, annealed and air cooled material has been examined by EBSD and the α_p separated from the α_s in the 2, 4 and 16 h samples on the basis on the Al-V composition difference. This separation of the α microstructural components is illustrated after 4 h of 'recrystallisation annealing' in Figure 9 and after 16 h in Figure 10. In the region observed of the 4 h sample, the α_p is mostly in only three (0002) orientations, A–A″. This orientation does account for some of the α_s, but a number of other α_s orientations (marked X) are present which are Burgers-related to the parent β orientation. Therefore in the 4 h sample the α_s that formed on cool-down took on a number of Burgers orientations.

In contrast in the 16 h sample, the α_s has exactly the same (0002) orientations as the parent α_p - no additional α orientations are visible in the α_s pole figures. This is even visible in the range of grain colours visible in the un-separated (all α) micrographs. Therefore after annealing is complete, a number of Burgers orientations were not observed, only those shared with the α_p.

This observation is consistent with the *in situ* measurements, which show strengthening of the α (0002) texture on heating associated with dissolution of the greater variety of α_s orientations, but no such softening associated with its re-precipitation on cooling. It is also consistent with the disappearance of the 45°texture components after 16 h that were observed in the lab. X-ray measurement *ex situ* after 2 h heat treatment.

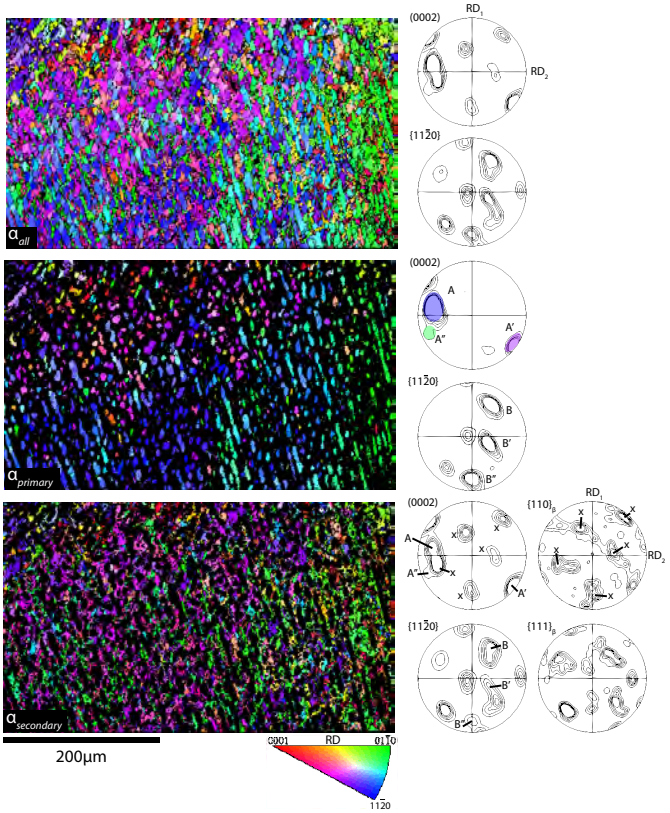

Fig. 9: EBSD measurements in the 50% rolled material after 4 h recrystallisation annealing showing the separation of the α_p and α_s components. Specific prior colony orientations A-A″ and B-B″ are denoted and (X) a number of other Burgers OR-related orientations in the α_s.

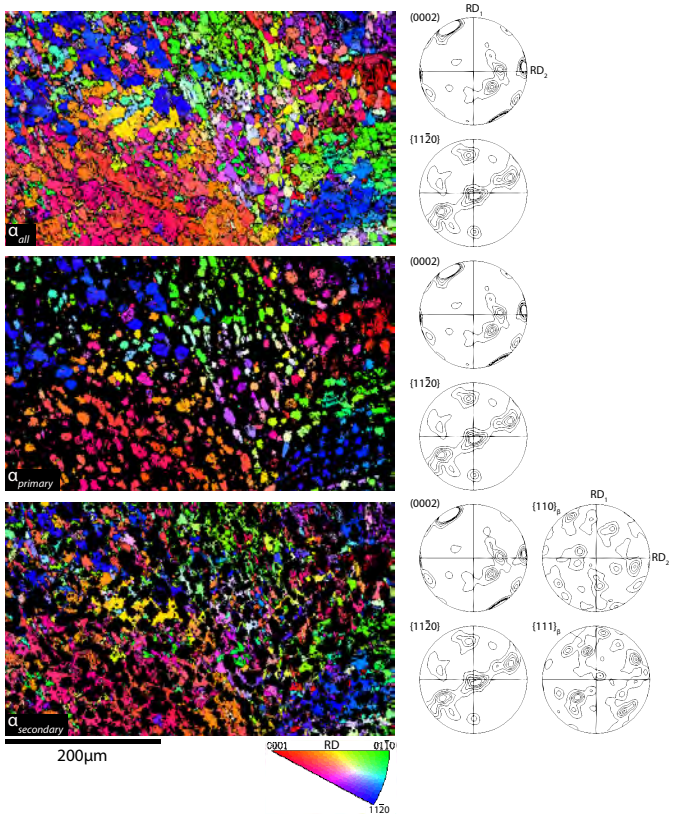

Fig. 10: EBSD measurements in the 50% rolled material after 16 h recrystallisation annealing showing the separation of the α_p and α_s components.

The 50% rolled material has been examined by EBSD, Figure 11, which also shows the differences between the primary α observed after 2 and 16 h annealing. In the as-rolled sample, the bending of an entire colony is visible (circled). In the 2 h sample, a remaining kinked α_p laths is still visible, which shows a significant rotation in orientation rotation concentrated in the curved / kinked region. The strain can then be measured from this local rotation (inset), with the associated geometrically necessary dislocations possibly providing a driving force for globularisation of the lath. In the 16 h sample, the α_p grains show much less intragranular misorientation (strain), indicating that the recrystallisation process was complete. Therefore the globularisation process gives rise to the texture strengthening of the α_p previously observed, as the range of α_p orientations present narrows due to the reconstruction of the kinked laths.

The mechanism by which the α_s orientations are selected therefore appears to depend on either or both of (i) the availability of nucleation sites (defects such as dislocations) in the β, which would reduce during annealing as the dislocation density reduces, or (ii) the nature of the α_p-β interface, which will presumably reduce in defect density as the α_p coarsening process becomes more dominant (large times) compared to α lath globularisation (early times). The first hypothesis can be inves-

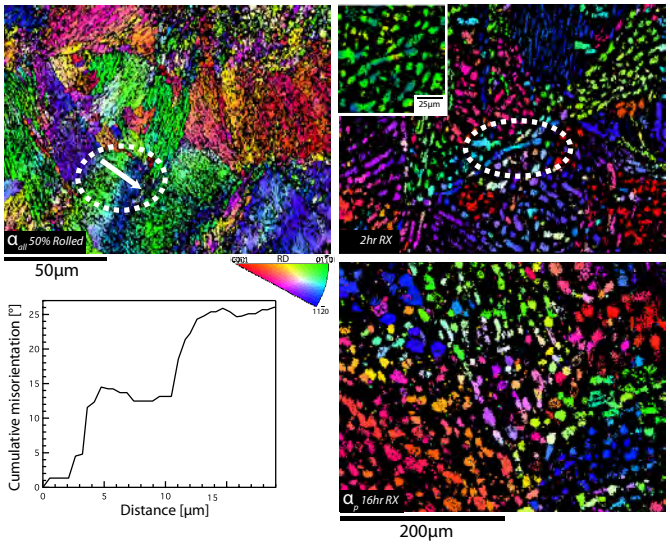

Fig. 11: EBSD measurements on the as- 50%rolled material (all points) and of the primary α in the 50% rolled material recrystallised for 2 h and 16 h. The rotation observed along a single colony in the as-rolled material is also shown.

tigated indirectly, from the β peak width evolution during heat treatment. Gaussian fitting of the whole-ring integration of the $\{110\}\beta$ peak at 3.58°showed that the β peak width remained approximately constant at $0.0094° \pm 0.0002°$ ($\delta d/d = 2.6 \times 10^{-3}$) throughout the hold at temperature, so within the resolution of the measurement no evolution could be observed. At room temperature, the β peak width was observed to be around 0.016°, higher than at temperature, which is presumably due to the production of defects on (re)precipitation of the α. These observations therefore do not support - but given the resolution, do not rule out - hypothesis (i). On balance, we prefer the interface defect density hypothesis (ii).

Whatever the actual mechanism, the consequence is clear - at short annealing times, several additional Burgers-OR related variants precipitate on cooling, whilst at long annealing times, the α_s share the orientation of the α_p. The difference between these two outcomes (variant diversity in the secondary α) is, of course, micromechanically important as it is becoming clear that the level of orientation homogeneity or self-organisation within so-called macrozones is important for the in-service fatigue performance obtained in the safety-critical applications for which $\alpha + \beta$ titanium alloys are often employed.

4. Conclusions

The evolution of texture in β-annealed Ti-6Al-4V during cross-rolling and so-called recrystallisation annealing has been studied using macro- and micro-texture measurements, both post mortem and using *in situ* synchrotron X-ray diffraction. In the microtexture measurements, separation of the α_p and α_s laths was achieved on the basis of their composition. The following conclusions can be drawn from this work.

1. During rolling at 950°C, the colony α laths kink during deformation and at higher strains, dynamic recrystallisation occurs, initially at prior β grain triple points. The α (0002) texture initially softens during rolling.
2. During subsequent reheating, initial dissolution of the α_s results in slight softening of the α texture. Globularisation of the α then results in further texture strengthening during the heat treatment, which continues at longer times as coarsening of the α_p becomes the dominant process.
3. The highly curved regions of the initial kinked α colonies contain significant orientation rotations. At the beginning of the heat treatment, during globularisation, these disapper, which is the mechanism behind texture strengthening during globularisation.
4. At relatively short annealing times, but after globularisation is largely complete, the α_s that forms on cooling takes on several of the possible Burgers OR orientations with the β, giving rise to a 45°component in the macroscopic (0002) texture.
5. At longer annealing times, the α_s that forms on cooling takes on the orientation of the surrounding α_p and therefore more organised macrozones are produced.

Acknowledgements

This work was funded by EPSRC under EP/E044700/1 and Rolls-Royce Plc., with material generously supplied by Timet UK Ltd. The support and encouragement of David Rugg at Rolls-Royce Plc. is gratefully acknowledged. Matthew Peel, John Daniels and Thomas Buslaps at ID15, ESRF provided invaluable assistance in performing the diffraction experiments, as did Tony Rollett at CMU and John Kallend at IIT on the analysis of texture data.

References

[1] R. Boyer, Mater Sci Eng A 213 (1996) 103–14.
[2] G. Lutjering, Mater Sci Eng A 243 (1998) 32–45.
[3] N. Stefansson, S. Semiatin, D. Eylon, Metall Mater Trans A 33 (2002) 3527–34.
[4] S. Semiatin, J. Brown, T. Brown, D. DeLo, T. Bieler, J. Beynon, Metall Mater Trans A 32 (2001) 1556–9.
[5] S. Semiatin, N. Stefansson, R. Doherty, Metall Mater Trans A 36A (2005) 1372–6.
[6] N. Stefansson, S. Semiatin, Metall Mater Trans A 34 (2003) 691–8.
[7] S. Semiatin, V. Seetharaman, I. Weiss, Mater Sci Eng A 263 (1999) 257–71.
[8] S. Semiatin, M. Corbett, P. Fagin, G. Salishchev, C. Lee, Metall Mater Trans A 37A (2006) 1125–36.
[9] M. Glavicic, J. Miller, S. Semiatin, Scr Mater 54 (2006) 281–6.
[10] L. Germain, N. Gey, M. Humbert, A. Hazotte, P. Bocher, A. Jahazi, Mater Characterization 54 (2005) 216–22.
[11] A. A. Salem, M. G. Glavicic, S. L. Semiatin, Mater Sci Eng A 494 (2008) 350–9.
[12] M. Bache, W. Evans, B. Suddell, F. Herrouin, Int J Fatigue 23 (2001) 153–9.
[13] M. Bache, W. Evans, Mater Sci Eng A 319 (2001) 409–14.
[14] M. Bache, W. Evans, V. Randle, R. Wilson, Mater Sci Eng A 257 (1998) 139–44.
[15] K. Le Biavant, S. Pommier, C. Prioul, Fatigue Fracture Eng Mater Structures 25 (2002) 527 – 45.
[16] L. Germain, N. Gey, M. Humbert, P. Bocher, M. Jahazi, Acta Mater 53 (2005) 3535–43.
[17] D. Rugg, M. Dixon, F. P. E. Dunne, J Strain Analysis 42 (2007) 269–79.

[18] A. Hammersley, S. Svensson, A. Thompson, Nucl Instrum Methods Phys A 346 (1994) 312–21.
[19] L. Lutterotti, S. Matthies, H. Wenk, A. Schultz, J. Richardson, J Appl Phys 81 (1997) 594–600.
[20] G. Ischia, H. Wenk, L. Lutterotti, F. Berberich, J Appl Crystallography 38 (2005) 377–80.
[21] I. Lonardelli, H. Wenk, L. Lutterotti, M. Goodwin, J Synchrotron Radiat 12 (2005) 354–60.
[22] H.-R. Wenk, in: Applications of Texture Analysis, Proceedings of the 15th international conference on textures of materials (ICOTOM15), Ceramic Trans. 201, Wiley, Hoboken, NJ, USA, (2009) 103 –13.
[23] J. Kallend, U. Kocks, A. Rollett, H. Wenk, Textures Microstructures 14 (1991) 1203–8.
[24] I. Bantounas, D. Dye, T. C. Lindley, Acta Mater 57 (2009) 3584 –95.
[25] I. Lonardelli, N. Gey, H.-R. Wenk, M. Humbert, S. C. Vogel, L. Lutterotti, Acta mater 55 (2007) 5718–27.
[26] J. Romero, M. Preuss, J. Q. da Fonseca, Acta Mater 57 (2009) 5501 –11.
[27] N. Gey, M. Humbert, Acta mater 50 (2002) 277–87.
[28] P. Ari-Gur, S. Semiatin, Mater Sci Eng A 257 (1998) 118–27.
[29] E. Shell, S. Semiatin, Metall Mater Trans A 30 (1999) 3219–29.
[30] J. Kearns, J Nucl Mater 299 (2001) 171–4.
[31] H. Moustahfid, N. Gey, M. Humbert, M.J. Philippe,Metall Mater Trans A 28 (1997) 51–61.
[32] S.V. Divinski, V.N. Dnieperenko, O.M. Ivahsin, Mater Sci Eng A 243 (1998) 201–5.